Japanese Journal of Applied Physics

REGULAR PAPER

Effect of source frequency and pulsing on the SiO_2 etching characteristics of dual-frequency capacitive coupled plasma

To cite this article: Hoe Jun Kim *et al* 2015 *Jpn. J. Appl. Phys.* **54** 01AE07

Japanese Journal of Applied Physics **54**, 01AE07 (2015) **REGULAR PAPER**
http://dx.doi.org/10.7567/JJAP.54.01AE07

Effect of source frequency and pulsing on the SiO_2 etching characteristics of dual-frequency capacitive coupled plasma

Hoe Jun Kim[1], Min Hwan Jeon[2], Anurag Kumar Mishra[1], In Jun Kim[3], Tae Ho Sin[3], and Geun Young Yeom[1,2*]

[1]*Department of Materials Science and Engineering, Sungkyunkwan University, Suwon 440-746, South Korea*
[2]*SKKU Advanced Institute of Nano Technology (SAINT), Sungkyunkwan University, Suwon 440-746, South Korea*
[3]*SEMES, Cheonan, Gyeonggi 331-810, Republic of Korea*
E-mail: gyyeom@skku.edu

Received February 6, 2014; revised May 13, 2014; accepted May 21, 2014; published online December 16, 2014

A SiO_2 layer masked with an amorphous carbon layer (ACL) has been etched in an Ar/C_4F_8 gas mixture with dual frequency capacitively coupled plasmas under variable frequency (13.56–60 MHz)/pulsed rf source power and 2 MHz continuous wave (CW) rf bias power, the effects of the frequency and pulsing of the source rf power on the SiO_2 etch characteristics were investigated. By pulsing the rf power, an increased SiO_2 etch selectivity was observed with decreasing SiO_2 etch rate. However, when the rf power frequency was increased, not only a higher SiO_2 etch rate but also higher SiO_2 etch selectivity was observed for both CW and pulse modes. A higher CF_2/F ratio and lower electron temperature were observed for both a higher source frequency mode and a pulsed plasma mode. Therefore, when the C 1s binding states of the etched SiO_2 surfaces were investigated using X-ray photoelectron spectroscopy (XPS), the increase of $C–F_x$ bonding on the SiO_2 surface was observed for a higher source frequency operation similar to a pulsed plasma condition indicating the increase of SiO_2 etch selectivity over the ACL. The increase of the SiO_2 etch rate with increasing etch selectivity for the higher source frequency operation appears to be related to the increase of the total plasma density with increasing CF_2/F ratio in the plasma. The SiO_2 etch profile was also improved not only by using the pulsed plasma but also by increasing the source frequency.

1. Introduction

As semiconductor devices are scaled down to nano scale levels for use in ultra scale integrated circuits, the etching of semiconductor devices is has become more difficult to satisfy more stringent requirements of etch characteristics such as etch profile, etch ratea, and etch selectivity.[1)] In particular, when high-aspect-ratio contacts (HARCs) are etched, plasma-process-induced damage (P2ID), such as pattern distortion and etch stops is observed, which can degrade the electrical performance of semiconductor devices.[2)] For the P2ID of HARCs, the electron shading effect caused by the isotropic flux of plasma electrons and the anisotropic flux of plasma ions, which result in negative and positive on the top and bottom of the HARC structure, respectively, is known to be the cause of pattern distortion.[3,4)]

To reduce the electron shading effect, various methods have been investigated and, among these, pulsed plasma techniques have been widely investigated by many research groups.[5)] Pulsed plasma is obtained by cyclically turning the radio frequency (rf) power on and off and is known to reduce electron shading by generating low-energy positive and negative ions during the pulse-off time.[6,7)] Samukawa and Mieno[8,9)] reported that negative ions generated during after-glow contribute to the reduction of positive surface charging at the bottom of the HARC during the plasma etching process. In terms of etch characteristics, Boswell and Henry[10)] reported that, although the etch rate under a pulsed plasma condition is lower than that under a continuous wave (CW) plasma condition, the etch selectivity under the pulsed plasma condition is much higher than that under the CW plasma condition. Plasmas generated by very high frequency (VHF) power sources in the range of 30–300 MHz have been extensively studied for reducing plasma damage. When a plasma is generated using a VHF source power, electrical charging damage is known to be reduced by decreasing the electron temperature (T_e) and plasma potential (V_p) of the plasma.[11,12)]

At present, for the etching of HARCs based on fluorocarbon plasmas, dual-frequency capacitive coupled plasmas (DF-CCPs) have also been extensively studied to control the plasma density and ion bombardment energy independently.[13,14)] When the source power of the DF-CCP was operated at a higher frequency, the etch profile was improved by the decreased number of ion collisions in the sheath caused by the decreased sheath thickness.[15)]

In this study, a DP-CCP composed of variable-frequency (13.56–60 MHz)/pulsed rf source power and 2 MHz CW rf bias power has been used in the experiment and the effects of the frequency and pulsing of the source rf power on the SiO_2 HARC etch characteristics were investigated using a C_4F_8/Ar gas mixture. In particular, we concentrated on the relationship of the SiO_2 etch characteristics with the change of reactive radicals such as CF_2 and F in the plasma.

2. Experimental procedure

The schematic diagram of the 300-mm-diameter DF-CCP etch system used in this study is shown in Fig. 1. The processing chamber and the bottom electrode were fabricated of anodized aluminum and the top electrode was fabricated of silicon supported by aluminum and a ceramic ring. The top silicon electrode surface was perforated for a uniform reactive gas flow over the substrate surface and the bottom electrode was cooled to room temperature by a chiller. The two electrodes were 20 mm apart. The top silicon electrode was connected to variable- and high-frequency power sources in the range of 13.56–60 MHz to control the plasma characteristics while the bottom electrode was connected to a low-frequency 2 MHz rf power source to control the ion bombardment energy. The chamber was evacuated by a turbomolecular pump (3200 l/s) backed by a dry pump. The process pressure was controlled automatically by adjusting the throttle valve.

A 600-nm-thick amorphous carbon layer (ACL) was used as a hardmask for SiO_2 HARC etching to maintain the critical dimension (CD) of the 2-μm-deep contact hole. The SiO_2

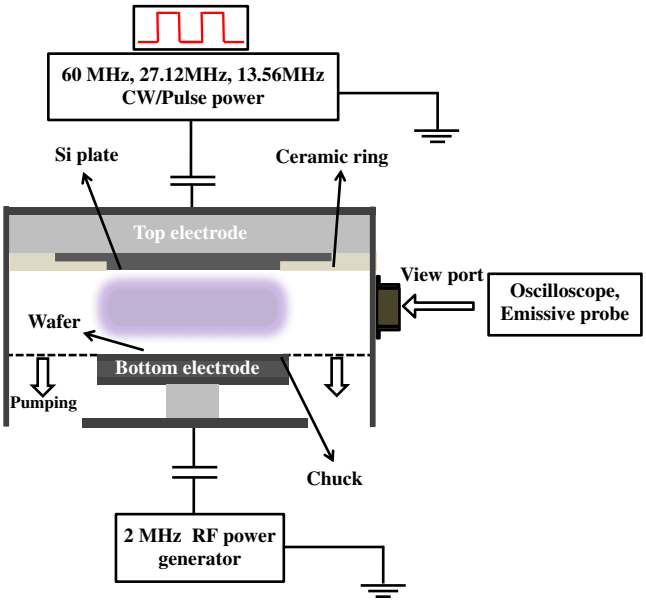

Fig. 1. (Color online) Schematic diagram of the DF-CCP used in the experiment. A 60, 27.12, or 13.56 MHz CW/pulse power was applied to the top electrode while a 2 MHz CW power was applied to the bottom electrode.

layer was etched by a CW/pulsed (duty percentage: 50%, 1 kHz) HF source frequency ranging from 13.56 to 60 MHz in an Ar/C_4F_8 plasma while biasing with 2 MHz CW rf power and while keeping the substrate temperature at room temperature.

The etch rates of SiO_2 and the ACL were measured using a step profilometer (Alpha Step 500) and the SiO_2 HARC etch profiles masked by the ACL were observed by field-emission scanning electron microscopy (FE-SEM; Hitachi S-4700). The change of the radical intensities of C_4F_8/Ar gas chemistry such as F, CF_2, and Ar was observed by optical emission spectroscopy (OES; Andor^{TM} Shamrock303). The C 1s binding states of the SiO_2 surfaces etched under various plasma conditions were observed using X-ray photoelectron spectroscopy (XPS; VG Microtech ESCA2000) by etching blank SiO_2 wafers. The characteristics of the substrate bias voltage and electron temperature during the pulse-on and pulse-off conditions for the pulsed plasma mode in addition to the CW plasma mode were measured using a high-voltage probe (Tektronix P6015A) and a laboratory-built emissive probe, respectively.

3. Results and discussion

Figures 2(a) and 2(b) show the etch rates of SiO_2 and the ACL and their etch selectivities, respectively, measured for source rf frequencies of 13.56, 27.12, and 60 MHz for the CW mode and pulsed mode (50% duty cycle with a pulsing frequency of 1 kHz). SiO_2 and the ACL were etched using a Ar (170 sccm)/C_4F_8 (40 sccm) gas mixture, an operating pressure of 40-mTorr, and a source rf power/bias rf power of 0.2 kW/1.2 kW. As shown in Fig. 2(a), the SiO_2 etch rate increased with the increase of rf frequency from 13.56 to 60 MHz both with and without pulsing even though the SiO_2 etch rate with the pulsing of a 50% duty cycle was about 20–30% lower than that etched with the CW mode. In the case of the ACL, the etch rate was not significantly changed with the increase of the source rf frequency. When the

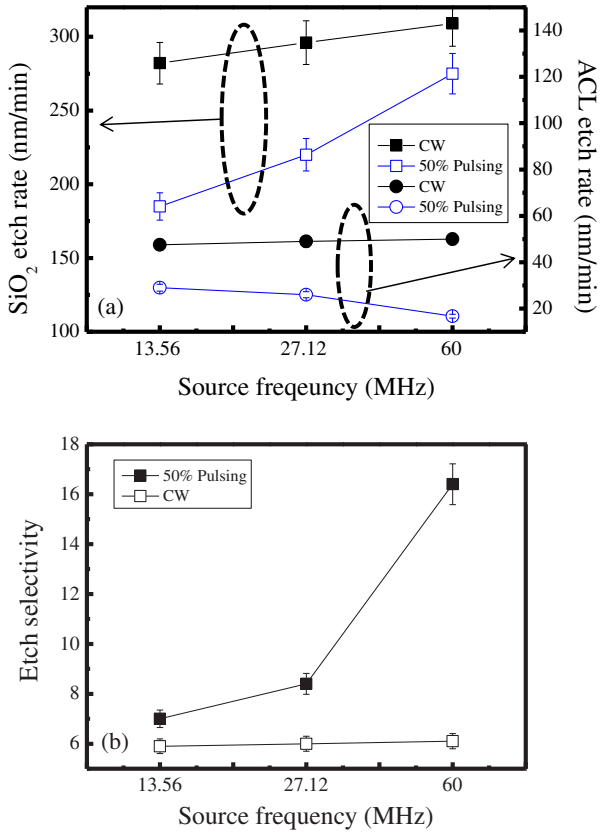

Fig. 2. (Color online) Etch rates of SiO_2 and ACL and etch selectivity of SiO_2 over ACL as a function of source frequency in the CW and pulsed plasma modes, (a) SiO_2 and ACL etch rate and (b) etch selectivity. A source rf power of 0.2 kW, 170/40 sccm of Ar/C_4F_8 at 40 mTorr, 50% duty ratio, and an rf power pulsing 1 kHz pulse frequency were used.

pulsing of a 50% duty cycle was used, the ACL etch rate was even decreased with an increase of source rf frequency in addition to the decrease of the ACL etch rate of about 30–50% by pulsing the rf power with a 50% duty cycle. Therefore, when the etch selectivities of SiO_2/ACL were measured, as shown in Fig. 2(b), the pulsed condition of a 50% duty cycle showed higher etch selectivity than the CW conditions and the etch selectivity was increased with the increase of source rf frequency for both the pulsed mode and the CW mode. In particular, the improvement of the etch selectivity of SiO_2/ACL with the source rf frequency was more significant for the pulsed plasma mode.

To investigate the reason for the differences in SiO_2 etch rates and etch selectivities, the radical intensities of Ar/C_4F_8 plasmas operated under different source rf frequency conditions and pulsed/CW modes were measured using OES. Figure 3 shows the optical emission intensity ratios of CF_2 (275.4 nm)/Ar (750.1 nm), F (703 nm)/Ar (750.1 nm),[16,17] and CF_2/F measured as a function of source rf frequency for the pulsed/CW modes shown in Fig. 2. As shown in Fig. 3, the intensity ratios of CF_2/Ar in the plasma were increased not only with the increase of source frequency but also by pulsing the plasma. The intensity ratios of F/Ar were slightly increased with the increase of source rf frequency; however, the pulsing the plasma decreased the F/Ar ratio at a given source rf frequency. The increase of source rf frequency from 13.56 to 60 MHz increased the intensity ratios of CF_2/F but pulsing the plasma with a 50% duty cycle

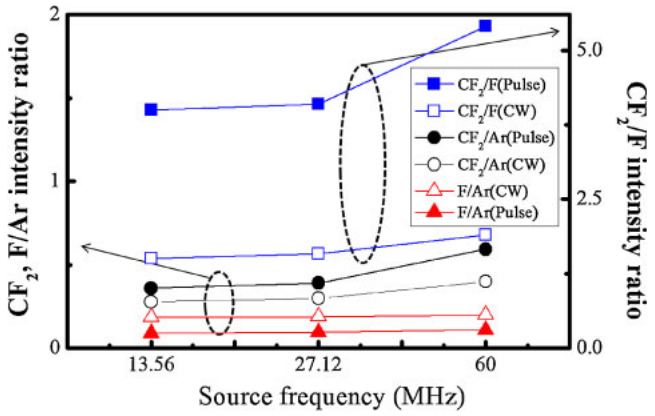

Fig. 3. (Color online) OES measurements of CF_2 and F radicals, and CF_2/F intensity ratio as a function of source frequency in the CW and pulsed plasma modes. The conditions are the same as those in Fig. 2.

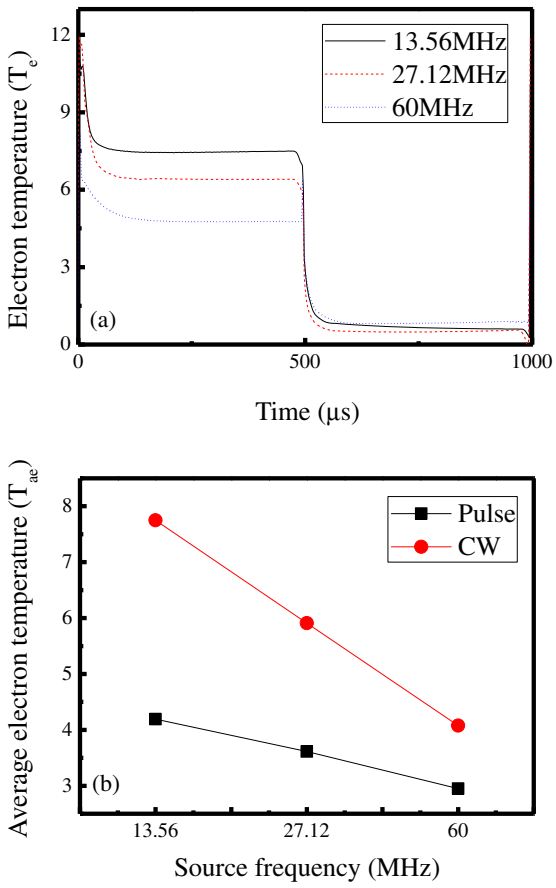

Fig. 4. (Color online) (a) Temporal electron temperature and (b) time-averaged electron temperature measured using an emissive probe. Ar gas was used and no bias power was applied. As the plasma conditions, a source rf power of 0.2 kW, 170 sccm of Ar at 40 mTorr, 50% duty ratio, and an rf power pulsing source with 1 kHz pulse frequency were used.

increased the CF_2/F ratio more significantly. In general, the increase of plasma source frequency increases the gas dissocation due to the increased plasma density in the plasma. Hence, the increased number of dissociated radicals such as CF_2 and F, observed with the increase of source rf frequency are believed to be related to the increased power consumption of the plasma. However, by pulsing the plasma, the dissociated radicals tend to recombine during the pulse-off period, and F appears to recombine with CF_x to form more CF_{x+1}. Therefore, as shown in the figure, by pulsing the plasma, the CF_2 radical intensity increased and F radical intensity decreased. The CF_x in the plasma tends to form a polymer layer on the substrate surface, even though SiO_2 can be etched by forming CO and SiF_x with CF_x, while F in the plasma tends to etch the ACL and SiO_2 nonselectively. Therefore, the increased SiO_2 etch rate and etch selectivity with the increase of source rf frequency are believed to be related to the increased gas dissociation of C_4F_8 with the increased CF_2/F ratio. The increased etch selectivity of SiO_2/ACL with decreasing SiO_2 etch rate for the pulsed condition is related to the increase in CF_x radicals with the decrease in F radicals by pulsing the plasmas. By operating at a higher source rf frequency, due to the increased SiO_2 etch rate with increased etch selectivity, a higher SiO_2/ACL etch selectivity could be observed for the pulsed plasma condition without decreasing the SiO_2 etch rate significantly.

Using an emissive probe, the temporal and time-averaged electron temperatures were measured as a function of rf frequency and the results are shown in Figs. 4(a) and 4(b), respectively. For the temporal electron temperature measurement, Ar was used and no bias power was applied. For the plasma conditions, source rf power of 0.2 kW, 170 sccm of Ar at 40 mTorr, 50% duty ratio, and source rf power pulsing with a pulse frequency of 1 kHz were used. As shown in Fig. 4(a), the electron temperature was stabilized instantly during the pulse-on condition for all the frequencies but a higher source rf frequency showed a lower electron temperature during the pulse-on time. Therefore, as shown in Fig. 4(b), not only the time-averaged electron temperature but also the temporal electron temperature was lower for the pulsed and higher frequency conditions. The higher CF_2/F ratios observed for pulsed and higher-rf-frequency conditions in Fig. 3 are believed to be related to the lower temporal and time-averaged electron temperature obtained by pulsing and using a higher source rf frequency.

Figures 5(a) and 5(b) show the temporal bias voltage and time-averaged bias voltage, respectively, measured on the substrate as a function of source rf frequency. In Fig. 5(b), the bias voltages measured in the CW mode are also shown. The process conditions were the same as those in Fig. 2 except for the bias power (0.6 kW of 2 MHz CW rf power was used). As shown in Fig. 5(a), during the source power pulse-on time, the bias voltage decreased and, during the source power pulse-off time, the bias voltage increased due to the decrease of plasma density. The bias voltages during the pulse-off time were the same; however, during the pulse-on time, due to the higher plasma density with the higher source rf frequency, the bias voltage was lower for a higher rf frequency. Therefore, the time-averaged bias voltage was higher for a lower source rf frequency condition and for the pulsed mode.

The surfaces of SiO_2 etched with Ar/C_4F_8 plasmas were investigated by XPS. Figures 6(a)–6(c) show the C 1s XPS narrow scan data of a SiO_2 surface obtained after the etching of SiO_2 for a similar etch depth of 700 nm with the different source rf frequencies of 13.56, 27.12, and 60 MHz, respectively, in the CW mode. As shown in the figure, carbon binding states related to C–C (284.9 eV), C–CF (287.9 eV), CF (289.8 eV), and CF_2 (291.5 eV) bonding were observed

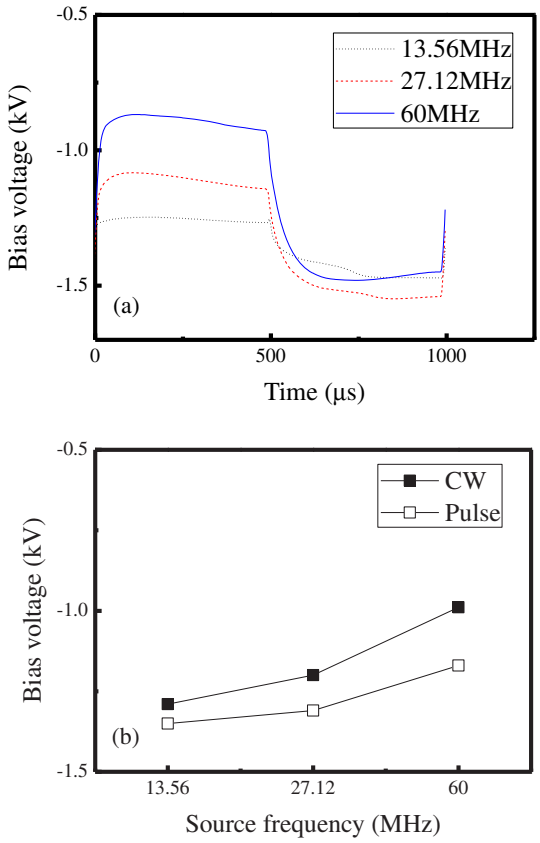

Fig. 5. (Color online) (a) Temporal bias voltage and (b) time-averaged bias voltage measured on the substrate as a function of source rf frequencies. The process conditions are the same as those in Fig. 2 except for the bias power (0.6 kW of 2 MHz CW rf power was used).

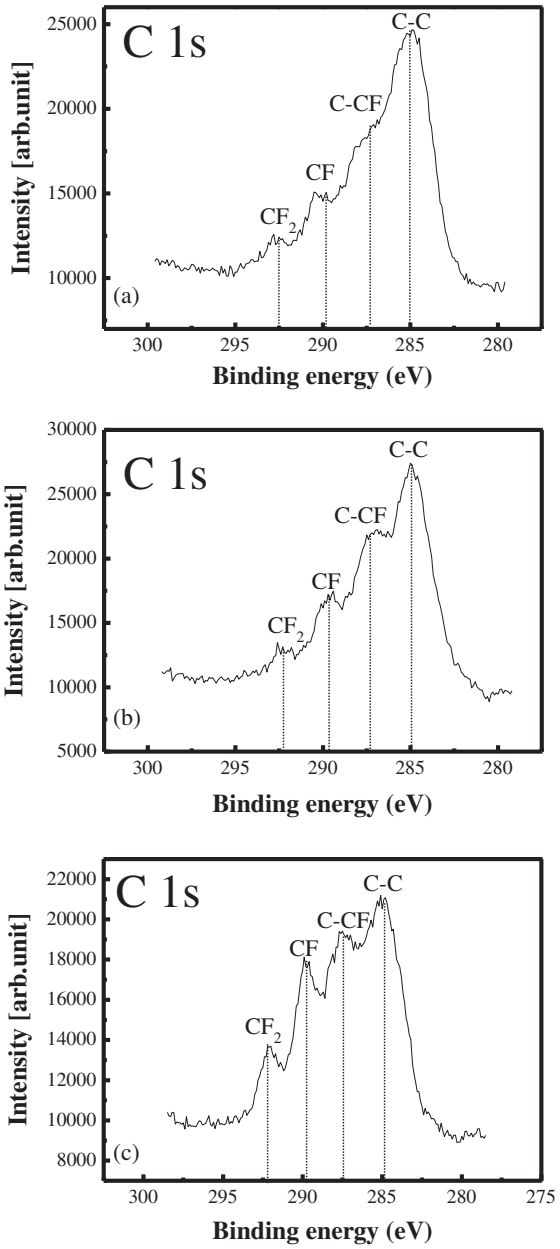

Fig. 6. XPS narrow scan C 1s data for SiO_2 surface after etching in the CW mode: (a) 13.56, (b) 27.12, and (c) 60 MHz. The other conditions are the same as those in Fig. 2.

and, as the source rf frequency is increased, the binding peak intensities related to C–CF, CF, and CF_2 bondings were increased while the C–C binding peak intensity decreased, possibly indicating the higher CF_x/F flux from the plasma as shown in Fig. 3.

Figures 7(a)–7(c) show the C 1s XPS narrow scan data of the SiO_2 surface obtained after the etching of SiO_2 under the same conditions as those in Fig. 6 with different source rf frequencies of 13.56, 27.12, and 60 MHz, respectively, but in the 50% duty pulse mode. For the pulsed plasma mode, as shown in Figs. 5(a)–5(c), the peak intensities related to C–CF, CF, and CF_2 bonding also increased with an increase of rf frequency similar to the CW condition in Fig. 6. In addition, comparison with Fig. 6 shows that pulsing the source power with the 50% duty pulse mode increased the bonding at C–CF, CF, and CF_2 on the etched SiO_2 surface, indicating increased CF_x/F flux from the plasma to the substrate at the same frequency by pulsing the plasma as also shown in Fig. 3.

Using SiO_2 wafers patterned with a 100-nm-wide ACL, the etch profiles were observed after the etching of SiO_2 as a function of rf source frequency for the CW and pulsed modes. The SiO_2 etch time was varied to maintain a similar SiO_2 etch depth. To maintain a similar SiO_2 etch depth, the etch time was decreased with increasing rf source frequency. It was also decreased for the CW mode compared to the pulsed mode due to the decreased SiO_2 etch rate with the decreased rf source frequency and with the pulsing as shown in Fig. 2. Figures 8(a)–8(c) show the SiO_2 etch profiles after etching in the CW mode for rf source frequencies of 13.56, 27.12, and 60 MHz, respectively. Similar to the results in Fig. 2, due to the increased etch selectivity, the remaining thickness of the ACL was slightly higher for the higher-frequency and pulsed mode conditions. In addition, a reduction of necking near the interface of the ACL and SiO_2 was observed with the increase of rf frequency. Figures 9(a)–9(c) show the SiO_2 etch profiles after the etching in the 50% duty pulse mode for the source rf frequencies of 13.56, 27.12, and 60 MHz, respectively. As shown in the figures, the pulsing, the profile was improved by decreasing the necking further at the interface of the ACL and SiO_2 and it had a more anisotropic etch profile.

4. Conclusions

In this study, SiO_2 masked with an ACL has been etched with

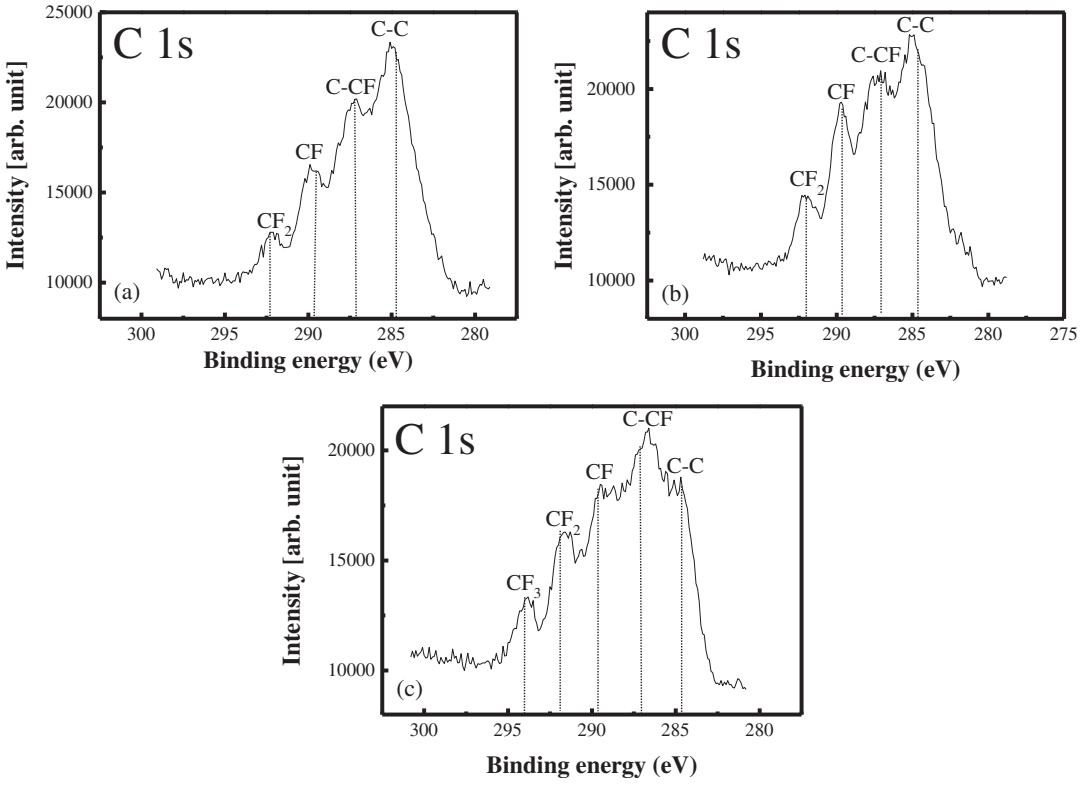

Fig. 7. XPS narrow scan C 1s data for SiO_2 surface after etching in the pulse mode (50% duty ratio and 1 kHz pulse frequency): (a) 13.56, (b) 27.12, and (c) 60 MHz. The other conditions are the same as those in Fig. 2.

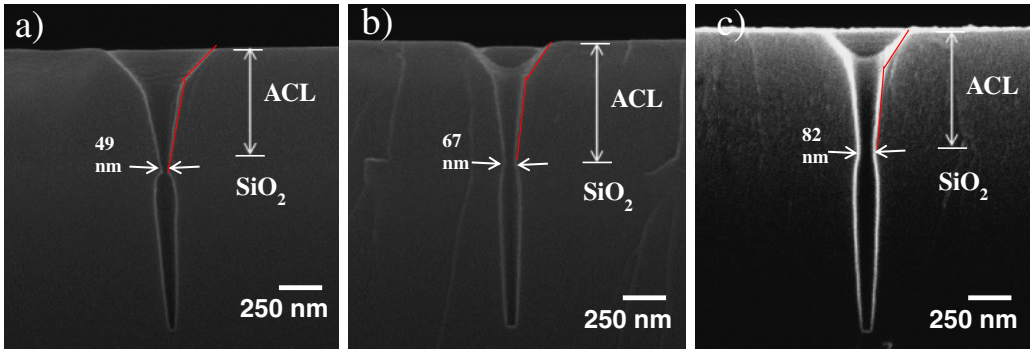

Fig. 8. (Color online) FE-SEM images of etched SiO_2 contact holes as a function of source frequency in the CW mode. (a) 13.56, (b) 27.12, and (c) 60 MHz. Process conditions: 0.2 kW source rf power, 40 mTorr, and 170/40 sccm Ar/C_4F_8.

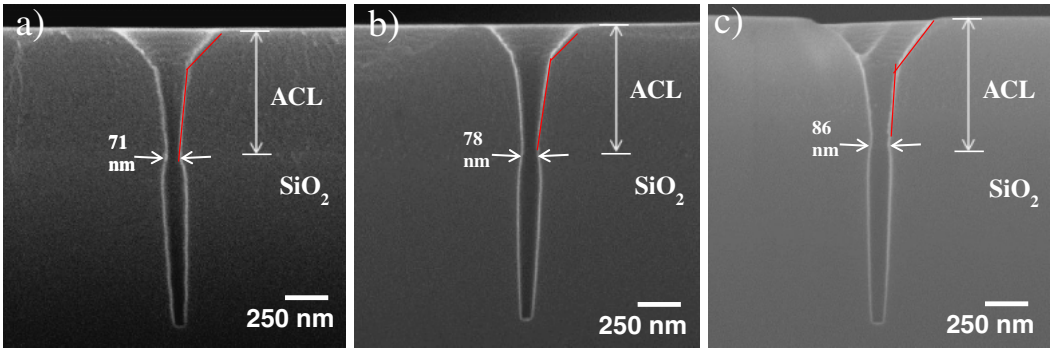

Fig. 9. (Color online) FE-SEM images of etched SiO_2 contact holes as a function of source rf frequency under the pulse condition: (a) 13.56, (b) 27.12, and (c) 60 MHz. Process condition: 0.2 kW of source rf power, 40 mTorr, and 170/40 sccm Ar/C_4F_8, 50% duty ratio, and source rf power pulsing with 1 kHz pulse frequency.

increasing rf source frequency from 13.56 to 60 MHz in the CW plasma mode and the pulse plasma mode (50% duty, 1 kHz) while applying 2 MHz CW bias power to the substrate. The effect of increasing source frequency on the SiO_2 etch characteristics in the CW and pulse plasma modes was investigated by using a C_4F_8-based gas in a DF-CCP system. With increasing source rf frequency, the SiO_2 etch rate and etch selectivity were increased for both the CW and pulse plasma modes. However, the etch selevtivity was more increased in the pulse plasma mode than in the CW plasma mode even though the SiO_2 etch rates were decreased by pulsing the plasma. The increased SiO_2 etch rates with the increase of rf frequencies for both the CW and pulse modes are believed to be related to the increased ionization and gas dissociation at the higher rf source frequencies. However, the increase of SiO_2 etch selectivity over ACL with increasing rf frequencies and by using the pulse mode instead of the CW mode is believed to be related to the increased CF_x/F flux to the substrate. OES and XPS results showed the increased CF_x/F ratio in the plasma and the CF_x bonding on the etched SiO_2 surface, respectively, with the increase of both the source rf frequency and by pulsing the source plasma. An improved of SiO_2 etch profile was also obtained with the increase of rf source frequency and by pulsing the source plasma. In particular, the significant improvement of the SiO_2 etch profile was observed at 60 MHz after the pulsed condition. Therefore, by combining the rf source frequency and pulsing, an anisotropic SiO_2 etch profile and high SiO_2 etch selectivity over the ACL can be obtained without significantly decreasing the SiO_2 etch rate.

Acknowledgements

This work was supported by the Industrial Strategic Technology Development Program (10041681, Development of fundamental technology for 10 nm process semiconductor and 10 G size large area process with high plasma density and VHF condition) funded by the Ministry of Knowledge Economy (MKE, Korea) and SEMES.

1) N. Ikegami, A. Yabata, T. Matsui, J. Kanamori, and Y. Horiike, Jpn. J. Appl. Phys. **36**, 2470 (1997).
2) J. Kim, K. S. Shin, W. J. Park, Y. J. Kim, C. J. Kang, T. H. Ahn, and J. T. Moon, J. Vac. Sci. Technol. A **19**, 1835 (2001).
3) K. Hashimoto, Jpn. J. Appl. Phys. **33**, 6013 (1994).
4) S. Banna, A. Agarwal, G. Cunge, M. Darnon, and E. Pargon, J. Vac. Sci. Technol. A **30**, 040801 (2012).
5) S. Samukawa and K. Terada, J. Vac. Sci. Technol. B **12**, 3300 (1994).
6) S. Samukawa, Appl. Phys. Lett. **68**, 316 (1996).
7) G. S. Hwang and K. P. Giapis, Jpn. J. Appl. Phys. **37**, 2291 (1998).
8) S. Samukawa, Appl. Phys. Lett. **64**, 3398 (1994).
9) S. Samukawa and T. Mieno, Plasma Sources Sci. Technol. **5**, 132 (1996).
10) R. W. Boswell and D. Henry, Appl. Phys. Lett. **47**, 1095 (1985).
11) S. Oda, Plasma Sources Sci. Technol. **2**, 26 (1993).
12) P. Chabert and N. Braithwaite, *Physics of Radio-Frequency Plasma* (Cambridge University Press, Cambridge, U.K., 2011) p. 177.
13) W. Tsai, G. Mueller, R. Lindquist, B. Frazier, and V. Vahedi, J. Vac. Sci. Technol. B **14**, 3276 (1996).
14) K. Bera, S. Rauf, K. Ramaswamy, and K. Collins, J. Appl. Phys. **106**, 033301 (2009).
15) M. J. Colgen, M. Meyyappan, and D. E. Murnick, Plasma Sources Sci. Technol. **3**, 181 (1993).
16) S. Samukawa and T. Mukai, J. Vac. Sci. Technol. A **17**, 2463 (1999).
17) J. H. Lee, B. S. Kwon, and N. E. Lee, Thin Solid Films **521**, 83 (2012).